DOI 10.1007/s11237-017-9502-1
*Theoretical and Experimental Chemistry, Vol. 53, No. 1, March, 2017 (Russian Original Vol. 53, No. 1, January-February, 2017)*

# INFLUENCE OF SBA-15 ZEOLITIZATION CONDITIONS ON STRUCTURAL-SORPTION AND ACIDIC PROPERTIES OF MICRO-MESOPOROUS ALUMINOSILICATES SBA-15/ZSM-5

**R. Yu. Barakov, N. D. Shcherban, P. S. Yaremov, S. M. Filonenko, V. V. Tsyrina, and V. G. Ilyin***

UDC 544.723.21; 544.478.02

*Partly zeolitized micro-mesoporous aluminosilicates SBA-15/ZSM-5 were synthesized by conversion of dry gel of template-containing SBA-15 in the presence of tetrapropylammonium hydroxide. They have a hexagonally ordered mesostructure and developed surface and mesoporosity for which the concentration and strength of the Brønsted and Lewis acid sites are higher than in AlSi-SBA-15. The formation of Brønsted acid sites of moderate strength in the samples with a low degree of zeolitization is due to the presence of ZSM-5 precursors as well as crystallites in the obtained aluminosilicates.*

***Key words**: micro-mesoporous aluminosilicate, SBA-15/ZSM-5, dry gel conversion, partial zeolitization, porosity, acidity.*

One of the most pressing tasks in the region of zeolite-like materials is the search and development of methods for obtaining micro-mesoporous (hierarchically-porous) aluminosilicates (MMAS) that combine the characteristics of zeolites (Zt) and mesoporous molecular sieves (MMS). Owing to the presence of developed mesoporosity and strong acid sites on the external surface (the mesopore surface) they exhibit high catalytic activity in conversion reactions (cracking, isomerization, etc.) of bulky molecules of organic substances for which the space in the micropores of traditional Zt is inaccessible [1, 2].

A promising approach for obtaining MMAS is zeolitization (crystallization directed toward formation of a zeolite phase) of an amorphous substance with a MMS framework of the SBA-15, MCF, MCM-41, and other types in the presence of a molecular template that promotes the formation of a zeolite structure [3]. Implementation of the zeolitization process by hydrothermal treatment (HTT) of mixtures (pH 9-10) containing AlSi-SBA-15 or AlSi-MCM-41 (previously impregnated with a molecular template, such as tetrapropylammonium hydroxide) at elevated temperatures (130-180 °C) destroys the MMS mesostructure, substantially reduces their mesoporosity, and leads to the formation of the larger crystals of Zt ZSM-5 [4]. In order to obtain X-ray amorphous (Zt precursors containing) and partially zeolitized MMAS having mesoporosity comparable with MMS the previously dried gel was therefore crystallized in nonaqueous solvents (e.g., glycerol) [5] or in the presence of the minimum amount of water (the dry gel conversion method) [6]. This makes it possible to reduce the proportion of dissolved

*Deceased.

L. V. Pisarzhevskii Institute of Physical Chemistry, National Academy of Sciences of Ukraine, Prospekt Nauky, 31, Kyiv 03028, Ukraine. E-mail: barakovchem07@rambler.ru. Translated from Teoreticheskaya i Éksperimental'naya Khimiya, Vol. 53, No. 1, pp. 58-66, January-February, 2017. Original article submitted February 6, 2017.

 

aluminosilicate, to reduce the mass transfer rate of the formed aluminosilicate particles, and to restrict the growth of Zt crystals, as a result of which zeolitization of only the surface layer of the framework of the mesoporous material can be expected [7].

In order to obtain zeolite-containing MMAS SBA-15/ZSM-5, having spatially ordered hexagonal mesostructures and developed mesoporosity, carbon–aluminosilicate composites C/AlSi-SBA-15 and also template-containing MMS of the SBA-15 type were subjected to zeolitization [8]. The presence of the carbon or the micellar template in the mesopores of the starting materials slows down destruction of their mesostructure during thermal steam or hydrothermal treatment. At the same time the accompanying blockage of the MMS mesopores can impede the processes leading to formation of the precursors and the Zt nuclei, as a result of which the strength of the acid sites in the obtained MMAS is reduced [9]. In order to obtain MMAS by conversion of the dry gel it is therefore important to optimize the composition of the reaction mixtures (a low concentration of the hydroxyl form of the molecular template, the optimum content of the molecular template in the MMS and of aluminum in its framework, and the absence of the alkali metal cations) and to use relatively mild conditions for thermal steam treatment (low temperature and short duration), which can lead to partial zeolitization of the MMS without destroying its mesostructure.

The aim of the present work is to clarify the effect of the zeolitization conditions of template-containing MMS SBA-15 on the structure-sorption characteristics of the obtained SBA-15/ZSM-5 MMAS.

## EXPERIMENTAL

As-synthesized MMS Si-SBA-15 samples with relatively thick walls (thickness 5.6 nm), obtained by the usual method [10] in a strongly acidic medium (pH 0.35), were used as starting materials. For the synthesis of the MMS we used a reaction mixture with the composition $1.0SiO_2$ : 0.016Pluronic P-123 : 5.5HCl : $152H_2O$ with the Pluronic P-123 triblock copolymer $[HO(CH_2CH_2O)_{20}(CH_2CH(CH_3)O)_{70}(CH_2CH_2O)_{20}H]$ and tetraethyl orthosilicate (TEOS) respectively as micellar template and silicon source. The reaction mixture was subjected to HTT at 100 °C for 24 h. The obtained Si-SBA-15 was washed with distilled water, dried at 100 °C for 24 h, and kept in a desiccator. For subsequent zeolitization (ZSM-5) the Si-SBA-15 was impregnated with an aqueous solution of the molecular template tetrapropylammonium hydroxide (TPAOH) containing hydroxoaluminate ions. To prepare this solution the aluminum source [aluminum isopropoxide $Al(i\text{-}PrO)_3$] in an amount corresponding to a molar ratio of Si/Al = 60 in the initial mixture was dissolved in 1.5 mL of a 0.05, 0.07, or 0.1 M aqueous solution of TPAOH for 2 h at room temperature under vigorous stirring. Then 0.2 g of the template-containing Si-SBA-15 was impregnated with 1.5 mL of the prepared TPAOH solution. The obtained mixture [composition $1SiO_2$ : $0.008Al_2O_3$ : (0.05-0.10)TPAOH : (51.5-52.0)$H_2O$] was stirred at room temperature for 1 h. The mixture was then dried at 60 °C for 24 h to evaporate water. The dried gel in a Teflon container was placed in an autoclave containing 1 mL of water and subjected to thermal steam treatment (TST) (with the samples in contact with the steam) at 100-120 °C for 16-144 h (Table 1, samples 1-8).

The standard procedure [11] was used to obtain the zeolite comparison sample (ZSM-5 with Si/Al = 50) in a reaction mixture not containing alkali metal cations. A reference sample of AlSi-SBA-15 (Si/Al = 50 in the initial reaction mixture) was obtained by a method similar to that one proposed in [12], in which a reaction mixture with the composition $1.0SiO_2$ : $0.01Al_2O_3$ : 0.016Pluronic P-123 : 5.5HCl : $152H_2O$ (pH 0.35), where the aluminum source was aluminum isopropoxide, was subjected to HTT at 100 °C for 24 h. Then, to introduce the aluminum into the SBA-15 framework the pH of the gel was raised to 7.5 by adding a 25% aqueous solution of ammonia, and the HTT was repeated at the same temperature and time.

All the obtained samples were washed with distilled water, dried at 100 °C, and calcined at 550 °C for 5 h (heating to the required temperature at 2 °C/min).

The phase composition of the obtained samples was determined on a Bruker D8 ADVANCE X-ray diffractometer with Cu$K_\alpha$ radiation. The average size of the ZSM-5 crystallites ($\beta_{cryst}$) was calculated using the Scherrer equation. The degree of zeolitization ($\alpha_{zt}$) of the investigated samples was estimated in comparison with Zt ZSM-5 by the change in the intensity ratios of the characteristic reflections for $2\theta$ = 23.0°, 23.8°, and 24.2°. The thermographic investigations were carried out on a Paulik–Paulik–Erdey Q-1000 derivatograph in the range of temperatures from room (20 °C) to 1000 °C (heating rate 10 °C/min). The IR spectra of the samples (in tablets with KBr, 1 : 100) were recorded on a Perkin Elmer Spectrum One Fourier spectrometer. Microphotographs of the sample were obtained on a Jeol JEM-2000FX transmission electron microscope (TEM). The Si and Al contents of the obtained samples were determined by energy-dispersive X-ray spectroscopy (with an adapter on the JEM-2000FX TEM). Nitrogen adsorption was measured by a volumetric method (77 K, up to 1 atm) on a

TABLE 1. Conditions of Synthesis, the Si/Al Ratio in the Samples, the Degree of Zeolitization, and the Size of Crystallites of the Obtained Samples

| Sample | TPAOH/Si in mixture | TST of mixture | | Si/Al | $\alpha_{zt}$ | $\beta_{cryst}$, nm |
|---|---|---|---|---|---|---|
| | | *T*, °C | τ, h | | | |
| 1 | 0.1 | 120 | 16 | 59 | – | – |
| 2 | 0.1 | 120 | 24 | 59 | 0.10 | 23 |
| 3 | 0.1 | 120 | 36 | 56 | 0.25 | 31 |
| 4 | 0.1 | 120 | 48 | 51 | 0.45 | 57 |
| 5 | 0.07 | 120 | 48 | 56 | <0.10 | 25 |
| 6 | 0.05 | 120 | 48 | 58 | – | – |
| 7 | 0.1 | 100 | 48 | 58 | – | – |
| 8 | 0.1 | 100 | 144 | 53 | 0.40 | 45 |

**Note.** τ is the duration of TST; $\alpha_{zt}$ is the degree of zeolitization; $\beta_{cryst}$ is the size of the ZSM-5 crystallites calculated using the Scherrer equation.

Sorptomatic 1990 analyzer for porous materials (Thermo Electron Corp.). The samples were first treated under vacuum ($p \leq 0.7$ Pa) at 350 °C for 5 h. The acid characteristics of the samples were investigated by the standard method of thermoprogrammed desorption of ammonia (TPDA) [13]. To characterize the nature, strength, and concentration of the acid sites we used the method of pyridine adsorption/desorption with IR spectroscopic control generally accepted for investigation of Zt and MMS [14-16]. We used the ad(de)sorption of 2,6-di-*tert*-butylpyridine (DTBPy) to determine the nature, strength, and concentration of acid sites localized on the mesopores surface, on the external surface area of the samples, and in the micropores of SBA-15 [16].

## RESULTS AND DISCUSSION

According to the data from X-ray diffraction (XRD) the initial sample of Si-SBA-15 has a spatially order hexagonal mesostructure that remains after the template removal. [In the small-angle region there are reflections at $2\theta = 0.8°$, 1.4°, and 1.6° corresponding to Miller indexes (100), (110), and (200) (Fig. 1a).]. The initial template-containing sample that was submitted to zeolitization contained 8 wt.% of water and 46 wt.% of micellar template (according to thermogravimetric analysis). The reference sample of AlSi-SBA-15 contained a more ordered mesostructure [five reflections in the small-angle region (Fig. 1a)] compared with Si-SBA-15, which can be explained by perfection of the mesostructure during repeated HTT of the reaction mixture (pH 7.5) used for the introduction of aluminum into the SBA-15 framework [12]. The Si-SBA-15 sample that had been impregnated with a solution of TPAOH (in which the aluminum source was dissolved) and submitted to TST (120 °C, 16 h, in the initial mixture Si/Al = 60, TPAOH/Si = 0.1) remained X-ray amorphous (Fig. 1a,b, sample 1). At the same time this sample contained the precursors Zt ZSM-5 (size <10 nm, which makes it impossible to detect them by XRD), as shown by the presence of a characteristic absorption band at 560 $cm^{-1}$ in the IR spectrum belonging to the asymmetric vibrations of the (alumino)siloxane bonds in the five-membered tetrahedra of $Si(Al)O_{4/2}$ in the secondary building units (SBU) of the ZSM-5 [17]. Thermal steam treatment of the dry gel at 120 °C for 24 h leads to partial zeolitization of the MMS SBA-15 (sample 2). [In the medium-angle region of the diffractogram of the sample there are low-intensity reflections characteristic of Zt ZSM-5 (Fig. 1b) with degree of zeolitization $\alpha_{zt} \approx 0.1$ and average crystallites size calculated using the Scherrer equation

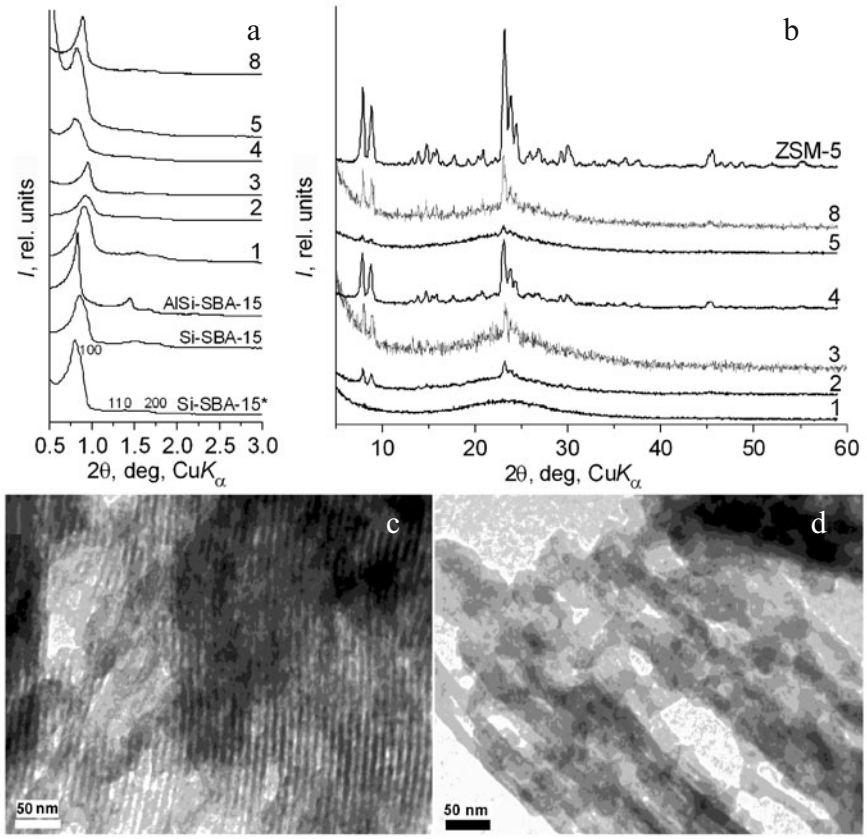


Fig. 1. Diffractograms of samples of MMAS SBA-15/ZSM-5, Si-SBA-15 (an asterisk indicates a template-containing sample), AlSi-SBA-15, and ZSM-5 in small-angle (a) and medium-angle (b) regions and TEM microphotographs of sample 2 (c, d).

$\beta_{cryst}$ = 23 nm (Table 1).] Partial zeolitization is also indicated by the presence of a characteristic absorption band at 550 $cm^{-1}$ in the IR spectrum of this sample. Sample 2 has a less ordered hexagonal mesostructure (Fig. 1a) than in the detemplated Si-SBA-15 and in sample 1, the diffractograms of which contain stronger small-angle reflections. The presence of the micellar template in the mesopores of the initial Si-SBA-15 sample thus allows its mesostructure to remain during the zeolitization process since crystallization of detemplated SBA-15 impregnated with a solution of the molecular template under analogous conditions (TST, 120 °C, 23 h) leads to significant destruction of its mesostructure [6]. Prolongation of TST at 120 °C to 36-48 h leads to increase in the degree of zeolitization of the MMAS [to 0.25 for sample 3, to 0.45 for sample 4 (Fig. 1b)]. Here the spatial ordering of the mesostructure in sample 4 is reduced. [There is only one reflection (100) in the small-angle region at 2θ = 0.9° (Fig. 1a).]

By reducing the TPAOH/Si ratio in the initial mixture (from 0.1 to 0.07) and realizing the TST of the dry gel at 120 °C for 48 h it is possible to obtain the partially zeolitized sample 5 (Table 1, $\alpha_{zt} < 0.1$, $\beta_{cryst}$ = 25 nm) with a more ordered mesostructure [three reflections in the small-angle region of the diffractogram of the sample (Fig. 1a)] than in sample 4 (Table 1, TPAOH/Si = 0.1). Zeolitization of the SBA-15 does not occur if the TPAOH/Si ratio in the initial mixture is reduced from 0.07 to 0.05 with subsequent TST of the dry gel (120 °C, 48 h) (Table 1, sample 6) as a result, probably, of the low concentration both of the structure-directing $TPA^+$ ions and of the $OH^-$ ions in the dry gel where ZSM-5 is not formed.

If the temperature of TST for the dry gel (TPAOH/Si = 0.1) is lowered from 120 to 100 °C, the duration of the process is increased; partial zeolitization of SBA-15 takes place after 144 h (Table 1, sample 8, $\alpha_{zt}$ = 0.4; with 48 h of TST zeolitization of SBA-15 does not occur, sample 7). The obtained sample 8 has a hexagonal mesostructure with a higher degree of ordering

TABLE 2. Characteristics of the Porous Structure of the Obtained Samples by Nitrogen Ad(de)sorption (77 K)

| Sample | $V_{micro}$, $cm^3/g$ | $V_{meso}$, $cm^3/g$ | $D_{meso}$, nm | $S_{meso}$, $m^2/g$ | $S_{BET}$, $m^2/g$ | $\lvert\Delta\mu_0\rvert$, kJ/mol |
|---|---|---|---|---|---|---|
| 1 | 0.08* | 0.84 | 7.3 ± 0.5 | 330 | 515 | 16.6 |
| 2 | 0.16 | 0.59 | 6.3 ± 0.9 | 280 | 630 | 29.2 |
| 3 | 0.14 | 0.56 | 6.5 ± 1.0 | 260 | 600 | 31.5 |
| 4 | 0.13 | 0.54 | 7.1 ± 1.2, 29.0 ± 4.6 | 230 | 530 | 34.6 |
| 5 | 0.12 | 0.50 | 6.1 ± 0.6 | 235 | 520 | 39.0 |
| 8 | 0.14 | 0.67 | 7.0 ± 0.9, 13.0 ± 1.1 | 275 | 605 | 33.0 |
| Si-SBA-15 | 0.15 | 0.81 | 6.3 ± 0.5 | 350 | 695 | 14.6 |
| AlSi-SBA-15 | 0.06 | 1.2 | 9.2 ± 0.5 | 400 | 530 | 10.7 |
| ZSM-5 | 0.16 | 0.05 | – | 20† | 375 | 64.5 |

**Note.** $V_{micro}$ = micropore volume; $V_{meso}$ = mesopore volume; $D_{meso}$ = mesopore diameter; $S_{meso}$ = mesopore specific surface area; $S_{BET}$ = total specific surface area; $\lvert\Delta\mu_0\rvert$ = initial adsorption potential of nitrogen; *micropore diameter for sample 1, Si-SBA-15, and AlSi-SBA-15 is ~0.8 nm; 0.55 nm for samples 2-5, 8, and ZSM-5; †external specific surface area of Zt ZSM-5.

(Fig. 1a) than sample 4 with a close degree of zeolitization (0.45). This is due to decrease in destruction of the mesostructure of SBA-15 under the conditions of TST at a lower temperature (100 °C).

If the duration of TST of the dry gel (TPAOH/Si = 0.1) containing a concentrated aqueous solution of TPAOH (~5.5 wt.% of water according to the TGA data) is increased from 16 to 48 h (at 120 °C) or from 48 to 144 h (at 100 °C), the Si/Al ratio in the samples decreases (Table 1), which agrees with data in [18]. This can be due to an increase in the concentration of dissolved silicate anions (aluminosiloxane bonds are more stable than siloxane bonds toward the action of strong bases), which are removed when the sample is washed with distilled water. The Si/Al ratio also decreases (Table 1) with an increase of the TPAOH/Si ratio in the dry gel (0.05 → 0.1, samples 4-6) or of the temperature of TST (100 → 120 °C, samples 4 and 7), which can be explained by the increased solubility of the silicate fragments of the MMAS.

Elements of the SBA-15 mesostructure (interplanar distance ~9 nm) can be distinguished on the TEM microphotographs of the partially zeolitized sample 2 (Fig. 1c). Zeolitization of SBA-15 is accompanied by partial destruction of its mesostructure (Fig. 1c,d).

The adsorption/desorption isotherms of nitrogen for the X-ray amorphous sample 1 and samples 2, 3, and 5 which have a low degree of zeolitization (0.1-0.25) belong to the IV type (according the IUPAC classification) and are typical for MMS having mesopores of fairly uniform size (Table 2, 6.1-7.3 nm). Samples 4 and 8 with a high degree of zeolitization (0.4-0.45) are characterized by the presence of structural mesopores (7.0-7.1 nm) characteristic for SBA-15 and also of secondary mesopores (13.0-29.0 nm) formed by gaps between the Zt ZSM-5 crystallites formed as a result of zeolitization of the amorphous substance of the MMS. In the obtained samples 1-5, 8 there are also micropores (Table 2), the volume of which is determined by the primary microporosity of the amorphous walls of the SBA-15 framework (micropores formed as a result of removal of the hydrophilic polyethylene oxide units of the template contained in the walls of the as-synthesized sample) and also by the presence of micropores in the ZSM-5 crystallites [19]. Thermal steam treatment of the dry gel (TPAOH/Si = 0.1) at 120 °C for 16 h leads to a decrease in the volume of the micropores in the walls of the framework of the obtained X-ray amorphous sample 1 compared with Si-SBA-15 (Table 2). This is due to "overgrowth" of the micropores as a result of additional condensation of the silanol and aluminol groups in the TST process. Sample 1 is characterized by a higher initial

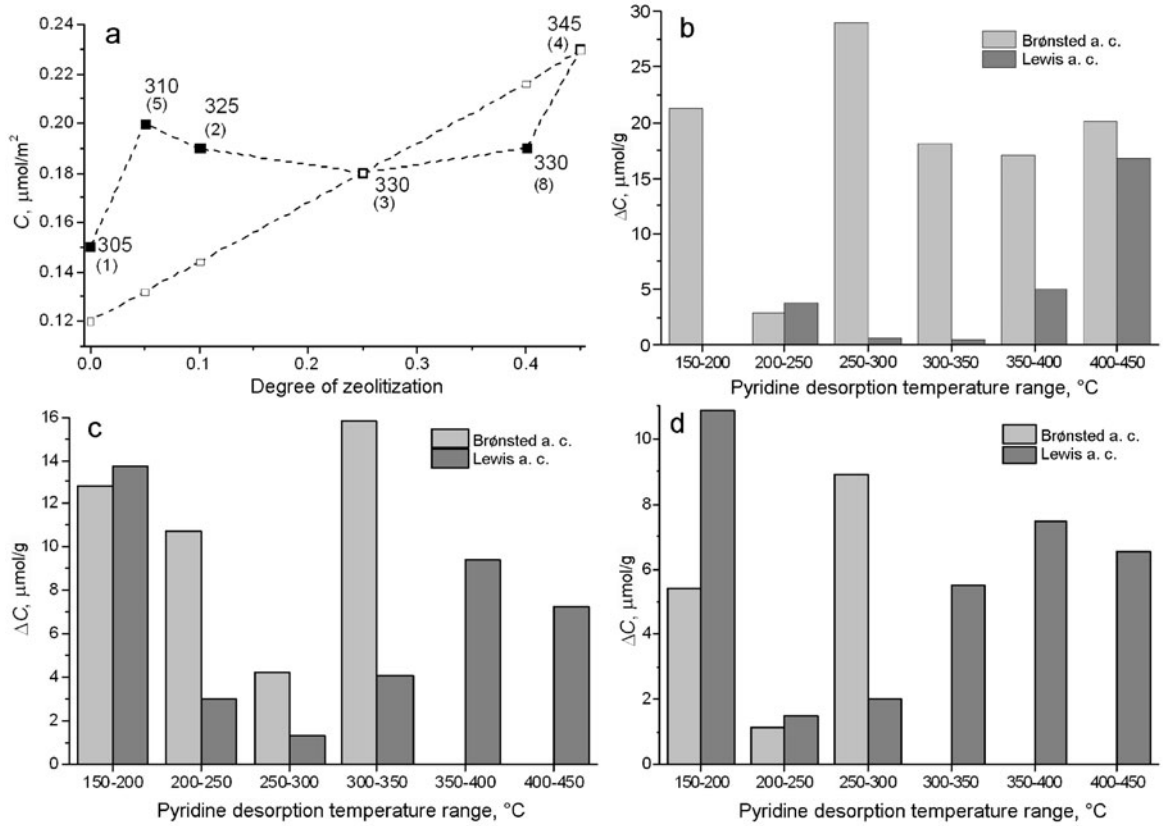


Fig. 2. a) Experimental (■) and calculated (□) changes of concentration of acid sites (by TPDA) with increase of the degree of zeolitization of MMAS (the temperatures for the desorption maximum of ammonia are shown, and the sample number is shown in parentheses). b-d) Histograms for the dependence of the amount of desorbed pyridine (related to unit sample mass) from Brønsted and Lewis acid sites on the desorption temperature ranges (according to data from pyridine ad(de)sorption with IR spectroscopic control) for ZSM-5-160 (b), sample 5 (c), and AlSi-SBA-15 (d).

adsorption potential for nitrogen $|\Delta\mu_0|$ than Si-SBA-15 (Table 2). This can be due to the presence in this sample of zeolite precursors characterized by higher values of $|\Delta\mu_0|$ as a result of bulk coverage of the micropores by molecules of the adsorbate [7]. The partially zeolitized sample 2 is characterized by smaller values for the volume and specific surface area of the mesopores and also for $S_{BET}$ compared with the detemplated initial MMS SBA-15 (Table 2). Increase in the duration of TST of the dry gel at 120 °C from 24 to 36-48 h (samples 2-4) leads to a decrease of the volume and specific surface area of the mesopores and also of $S_{BET}$ of the aluminosilicate (Table 2), and this is due to disordering of the mesostructure of the MMS as a result of zeolitization. The larger size of the structural mesopores in sample 4 compared with sample 2 can be explained by partial dissolution of the walls of the SBA-15 framework during zeolitization. Here increase in the degree of zeolitization of the MMAS (to 0.45) and increase in the size of the crystallites in sample 4 (Table 1) are accompanied by increase of the initial adsorption potential of nitrogen (Table 2). The smaller value of $V_{micro}$ in sample 4 compared with sample 2 can be explained by involvement of the substance of the amorphous walls of the SBA-15 framework in the zeolitization process. If the TPAOH/Si ratio in the dry gel is reduced from 0.1 to 0.07 (samples 4 and 5), the degree of spatial ordering of the mesostructure of the MMAS is increased, and the degree of uniformity in sizes of the structural mesopores of the aluminosilicate is raised (Table 2). By lowering the temperature of zeolitization of the SBA-15 (120 → 100 °C) it is possible to obtain a partially zeolitized sample 8 that has a more ordered mesostructure than sample 4 and is consequently characterized by higher values for the volume, specific surface area, and $S_{BET}$ and higher mesopore size uniformity (Table 2, samples 4 and 8).

According to the data from TPDA, the obtained partially zeolitized MMAS (samples 2-5, 8, Si/Al = 51-59) contain medium-strength and strong acid sites [$NH_3$ desorption maximum ≥300 °C (Fig. 2a)]. The total concentration of acid sites in these samples (102-117 μmol/g) is close to ZSM-5 (136 μmol/g, ammonia desorption maximum 440 °C, Si/Al = 50). The MMAS samples have higher strengths and higher concentrations of acid sites compared with amorphous AlSi-SBA-15 (Si/Al = 55, concentration 61 μmol/g, desorption maximum 300 °C). The large concentration of acid sites ($NH_3$ desorption maximum 300-305 °C) in the X-ray amorphous sample 1 (75 μmol/g) compared with AlSi-SBA-15 can be explained by the higher concentration of tetrahedrally coordinated aluminum in the Zt precursors in the obtained MMAS than in the amorphous AlSi-SBA-15 framework, which is confirmed by the data in [5]. The higher surface concentration of acid sites in sample 1 (0.15 μmol/$m^2$) compared with AlSi-SBA-15 (0.12 μmol/$m^2$) also indicates the presence of Zt precursors in the MMAS sample. Increase of the degree of zeolitization of SBA-15 from 0.05 to 0.45 is accompanied by an increase of the strength of the acid sites in MMAS (increase of the temperature of ammonia desorption maximum, samples 2-5, 8) and also by some increase of their concentration (Fig. 2a).

By investigating the adsorption/desorption of pyridine it was possible to detect Brønsted acid sites (B sites, concentrations 43-48 μmol/g) and Lewis acid sites (L sites, 64-73 μmol/g) in the obtained partially zeolitized MMAS samples 2, 4, 5, and 8. To estimate the strength of the acid sites in the samples the data from the pyridine adsorption/desorption method with IR spectroscopic control were presented in the form of histograms: the dependence of the amount of desorbed pyridine [related to unit mass of sample ($\Delta C$)] from the Brønsted and Lewis acid sites (determined from the difference in the concentrations of the acid sites corresponding to the two closest desorption temperatures) on the desorption temperature range (Fig. 2b-d). The thermodesorption maxima correspond to the temperature ranges in which the largest amount of pyridine is desorbed. Depending on the value of the pyridine desorption maximum, it is possible to identify conditionally the weak (pyridine desorption maximum up to 250 °C), medium-strength (desorption maximum from 250 to 350 °C), and strong (desorption maximum >350 °C) acid sites. According to this, the Zt ZSM-5 has three types of Brønsted acid sites (Fig. 2b): weak (desorption maximum at 150-200 °C), medium strength (desorption maximum at 250-300 °C), and strong (desorption maximum at 400-450 °C) and also weak (desorption maximum at 200-250 °C) and strong (desorption maximum at 400-450 °C) Lewis acid sites. Sample 5 with a small degree of zeolitization (<0.1), containing Zt ZSM-5 nuclei, is characterized by greater strength (Fig. 2c, pyridine desorption maxima at 150-200 °C and 300-350 °C) and concentration of Brønsted acid sites (44 μmol/g) and a higher concentration of Lewis acid sites (73 μmol/g) compared with AlSi-SBA [B sites 15 μmol/g, desorption maxima at 150-200 °C and 250-300 °C (Fig. 2d); L sites 39 μmol/g]. The partially zeolitized sample 5 is also characterized by a higher ratio of concentrations of Brønsted acid sites to Lewis sites ($C_B/C_L$ = 0.6) compared with AlSi-SBA-15 ($C_B/C_L$ = 0.4), which can be due to the larger proportion of Al atoms with tetrahedral coordination in sample 5 [20]. Increase of the degree of zeolitization to 0.1 (sample 2) leads to an increase in the strength of the Lewis acid sites in the sample (desorption maximum shifted from 350-400 °C to 400-450 °C, concentration 68-73 μmol/g). Further increase in the degree of zeolitization of SBA-15 to 0.40-0.45 (samples 4, 8) is accompanied by an increase in the strength of the Brønsted acid sites (desorption maximum at 350-400 °C, concentration 43-48 μmol/g) and also of the $C_B/C_L$ ratio (from 0.6 to 0.7). Unlike samples 2 and 5 with a low degree of zeolitization, samples 4 and 8 are characterized by the presence not only of weak and strong Lewis acid sites but also of acid sites of medium strength (desorption maximum 250-300 °C for sample 4, 300-350 °C for sample 8). Consequently, increase of the duration of TST of the dry gel (to 48 h at 120 °C or to 144 h at 100 °C) leads to the appearance in samples 4 and 8 of medium-strength Lewis acid sites that can be defects in the SBA-15 structure or ZSM-5 crystallites (e.g., tricoordinated Al atoms) [21]. The higher values of the high-temperature maxima for the pyridine desorption from L sites than from B sites in samples 2, 4, 5, and 8 and AlSi-SBA-15 can be due not to the greater strength of the L sites but to the lower thermal stability of the Brønsted acid sites, which can change to L sites under the conditions of dehydroxylation at elevated desorption temperatures (300-450 °C).

By investigating the adsorption/desorption of 2,6-di-*tert*-butylpyridine (DTBPy) it was possible to determine the nature, concentration, and strength of the acid sites presented on the surface of the MMAS mesopores and on the external surface of the ZSM-5 crystallites and also in the micropores of SBA-15 ($D_{micro} \approx 0.8$ nm) since the ZSM-5 micropores ($D_{micro}$ = 0.55 nm) are inaccessible to DTBPy molecules (kinetic diameter of DTBPy 0.8 nm) [22]. According to this method the Brønsted (16-32 μmol/g) and Lewis acid sites are located on the mesopore surface of the obtained samples 2, 4, 5, and 8 and also in the micropores of the framework walls. Steric hindrances arising from the presence of the *tert*-butyl groups can prevent

interaction of the DTBPy with the L sites, which makes it impossible to determine the concentration of Lewis acid sites quantitatively by this method [23]. The Zt ZSM-5 with a small external specific surface area (20 $m^2/g$) is characterized by an insignificant concentration of acid sites accessible to DTBPy molecules (4 μmol/g). The partially zeolitized sample 2 with a developed mesopore surface (280 $m^2/g$) has higher concentration and strength of Brønsted acid sites (31 μmol/g, desorption maxima at 200-250 and 350-400 °C) and Lewis acid sites (concentration determined from the integral intensity of the absorption band at 1466 $cm^{-1}$, DTBPy fully desorbed at 450 °C) compared with AlSi-SBA-15 (B sites 26 μmol/g, desorption maxima at 150-200 °C and 250-300 °C, DTBPy fully desorbed from L sites at 350 °C). With an increase in the degree of zeolitization from 0.1 (sample 2) to 0.4 (sample 8), the strength of the Brønsted acid sites increases (desorption maxima at 250-300 °C, 350-400 °C). The ratio of the concentrations of Brønsted acid sites, determined from the adsorption/desorption of DTBPy and pyridine (the "accessibility coefficient"), amounts to 0.72 and 0.74 respectively for samples 2 and 8. This shows that most of the B sites in these samples, having a developed mesopore surface of 275-280 $m^2/g$, are accessible to bulky molecules. The partially zeolitized samples 4 and 5 with mesopore specific surface area of 230-235 $m^2/g$ have a somewhat lower concentration of Brønsted acid sites accessible to DTBPy molecules (16-22 μmol/g) compared with AlSi-SBA-15 (26 μmol/g, $S_{meso}$ = 400 $m^2/g$) but are superior to MMS in the strength of these sites (DTBPy desorption maximum at 350-400 °C for sample 4, at 300-350 °C for sample 5, and at 250-300 °C for AlSi-SBA-15).

To reveal the differences in the acidity of MMAS from a mechanical mixture of Zt and MMS the experimental values of the concentration of medium acid sites and strong acid sites ($NH_3$ desorption maximum at ≥300 °C, TPDA) of partially zeolitized samples 2-5 and 8 were compared with the corresponding calculated values obtained from the assumption that the individual phases Zt and MMS are present in the MMAS. The calculated values for the concentrations of medium and strong acid sites were determined using the equation $C_{calc} = \alpha_{zt}C_{zt} + (1 - \alpha_{zt})C_{mms}$, where $\alpha_{zt}$ is the degree of zeolitization of the MMS; $C_{zt}$ is the concentration of strong acid sites in the Zt (0.36 μmol/$m^2$); $C_{mms}$ is the concentration of acid sites of medium strength in AlSi-SBA-15 (0.12 μmol/$m^2$). The surface concentration of acid sites (in μmol/$m^2$) in the obtained samples of MMAS is larger than the calculated value for $\alpha_{zt}$ from 0 to 0.25. However the surface concentration of acid sites is somewhat lower than the calculated values or corresponds them at the higher degree of zeolitization (0.25-0.45). It can be supposed that with relatively low values for the degree of zeolitization (up to 0.25) the fact that the concentration of acid sites is higher than the calculated values results from the presence in the MMAS samples, apart from ZSM-5 crystallites, of the X-ray amorphous Zt precursors (the SBU of Zt) that have a higher concentration of acid sites compared with the amorphous framework of AlSi-SBA-15 [24, 25]. With higher degrees of zeolitization (0.25-0.45) the lower values of the surface concentration of acid sites in the MMAS samples compared with the calculated values can be due to the higher degree of dispersion (smaller size) of the Zt crystals in the MMAS samples (Table 1) in relation to the reference sample Zt ZSM-5 (average size ~1.5 μm). The differences in the values of the maxima for the desorption of pyridine from the Brønsted acid sites for samples 2 and 5 from ZSM-5 and AlSi-SBA-15 (Fig. 2b-d) and particularly the presence of maxima for the desorption of pyridine from these sites at 300-350 °C for MMAS, which are absent for the reference samples, also point out the nonadditivity of the acidity characteristics of the MMAS and can indicate the presence of X-ray amorphous precursors of Zt in samples with a low degree of zeolitization.

Partially zeolitized micro-mesoporous aluminosilicate SBA-15/ZSM-5 were, thus, obtained by conversion of a dry gel of template-containing mesoporous molecular sieve SBA-15 in the presence of tetrapropylammonium hydroxide (TPAOH/Si = 0.07-0.1) in a relatively low-temperature thermal steam treatment (100-120 °C). The obtained aluminosilicates have a hexagonally ordered mesostructure, are characterized by a developed surface and mesoporosity, and contain Brønsted and Lewis acid sites with higher concentrations and strength than for AlSi-SBA-15. By lowering the temperature of thermal steam treatment of the dry gel to 100 °C it is possible to obtain zeolitized aluminosilicates with a higher concentration of acid sites on the mesopore surface compared with aluminosilicates obtained at 120 °C. The nonadditivity of the acidity characteristics of the micro-mesoporous aluminosilicates with a low degree of zeolitization (0.05-0.2) indicates that they also contain ZSM-5 precursors in addition to the crystallites.

## REFERENCES

1. K. Na and G. A. Somorjai, *Catal. Lett.*, **145**, No. 1, 193-213 (2015).

2. W. Schwieger, A. G. Machoke, T. Weissenberger, et al., *Chem. Soc. Rev.*, **45**, No. 12, 3353-3376 (2016).
3. D. P. Serrano, J. M. Escola, and P. Pizarro, *Chem. Soc. Rev.*, **42**, No. 9, 4004-4035 (2013).
4. S. Habib, F. Launay, M. A. Springuel-Huet, et al., *J. Porous Mater.*, **16**, No. 3, 349-359 (2009).
5. K. R. Kloetstra and J. C. Jansen, *Chem. Commun.*, No. 23, 2281-2282 (1997).
6. V. Pashkova, E. Włoch, A. Mikołajczyk, et al., *Catal. Lett.*, **128**, Nos. 1/2, 64-71 (2009).
7. N. D. Shcherban and V. G. Ilyin, *Teor. Éksp. Khim.,* **51**, No. 6, 331-349 (2015). [*Theor. Exp. Chem.*, **51**, No. 6, 339-357 (2016) (English translation).]
8. J. Wang, A. Vinu, and M.-O. Coppens, *J. Mater. Chem.*, **17**, No. 40, 4265-4273 (2007).
9. S. Habib, F. Launay, M.-A. Springuel-Huet, et al., *New J. Chem.*, **30**, No. 8, 1163-1170 (2006).
10. D. Zhao, J. Feng, Q. Huo, et al., *Science*, **279**, No. 5350, 548-552 (1998).
11. H. Jin, M. Bismillah Ansari, and S.-E. Park, *Chem. Commun.*, **47**, No. 26, 7482-7484 (2011).
12. S. Wu, Y. Han, Y. C. Zou, et al., *Chem. Mater.*, **16**, No. 3, 486-492 (2004).
13. S. Hu, J. Shan, Q. Zhang, et al., *Appl. Catal. A*, **445**/**446**, 215-220 (2012).
14. C. A. Emeis, *J. Catal.*, **141**, No. 2, 347-354 (1993).
15. D. P. Serrano, R. A. García, G. Vicente, et al., *J. Catal.*, **279**, No. 2, 366-380 (2011).
16. C. Jo, R. Ryoo, N. Žilková, et al., *Catal. Sci. Technol.*, **3**, No. 8, 2119-2129 (2013).
17. C. E. A. Kirschhock, R. Ravishankar, F. Verspeurt, et al., *J. Phys. Chem. B*., **103**, No. 24, 4965-4971 (1999).
18. M. B. Yue, L. B. Sun, T. T. Zhuang, et al., *J. Mater. Chem.*, **18**, No. 17, 2044-2050 (2008).
19. N. D. Lysenko, V. G. Il'in, and P. S. Yaremov, *Teor. Éksp. Khim.,* **47**, No. 4, 246-251 (2011). [*Theor. Exp. Chem.*, **47**, No. 4, 257-263 (2011) (English translation).]
20. R. Barakov, N. Shcherban, P. Yaremov, et al., *J. Porous Mater.*, **23**, No. 6, 1619-1632 (2016).
21. S. Habib, F. Launay, H. El Zakhem, et al., *Mater. Res. Bull.*, **48**, No. 3, 1288-1295 (2013).
22. K. Kim, R. Ryoo, H.-D. Jang, and M. Choi, *J. Catal.*, **288**, 115-123 (2012).
23. H. Knözinger, *Elementary Reaction Steps in Heterogeneous Catalysis*, R. W. Joyner, R. A. van Santen (eds.), Springer, Dordrecht, Netherlands, (1993), Vol. 398, pp. 267-285.
24. A. Torozova, P. Mäki-Arvela, N. D. Shcherban, et al., *Catal. Struct. React.*, **1**, No. 3, 146-154 (2015).
25. R. Barakov, N. Shcherban, P. Yaremov, et al., *J. Mater. Sci.*, **51**, No. 8, 4002-4020 (2015).